Supporting Information
To

Impacts of Hematite Nanoparticle Exposure on Biomechanical, Adhesive, and Surface Electrical Properties of *E. coli* Cells

Wen Zhang[1], Joseph Hughes[1,2,3] and Yongsheng Chen[1*]

[1]School of Civil and Environmental Engineering, Georgia Institute of Technology, Atlanta, Georgia, 30332. [2]School of Materials Science and Engineering, Georgia Institute of Technology, Atlanta, Georgia, 30332, [3]College of Engineering, Drexel University, Philadelphia, PA 19104

[*]To whom correspondence should be addressed:

Dr. Yongsheng Chen,

Department of Civil and Environmental Engineering

Georgia Institute of Technology, Atlanta, Georgia, 30332

E-mail: yongsheng.chen@ce.gatech.edu;

Phone: (+1) 404-894-3089; Fax: 404-894-2278

[*]Corresponding author phone: (+1) 404-894-3089, Fax: (+1) 404-894-2278, and e-mail: yongsheng.chen@ce.gatech.edu.

This supporting information includes the following sections:

S1. Justification of the loading force magnitude in the AFM force measurement

A maximum loading force of 4 nN was chose to push the tip against the cell surface to measure the surface hardness. We intend to measure the indentation for the tip-membrane interactions instead of measuring the interaction forces on the outside layer of the cell (e.g., surface appendages–pili or surface brushes). This is partly because the physical disruption from hematite exposure likely altered the mechanical properties of the cell membrane (2, 6, 7, 9, 11), which is beneath the tightly packed lipopolysaccharide (LPS) molecules and mainly determines the mechanical response. More importantly, through changing the adhesiveness or mechanical properties, the sorption of hematite NPs could disrupt the integrity of the cytoplasm membrane structure (4). Thus, quantifying the membrane property is more relevant in this study. Since Velegol and Logan indicated that in the nonlinear regime the tip contacted the outer membrane but had yet to encounter the stiff peptidoglycan layer (12), we applied a relatively high loading force (~nN) in an effort to engage the tip with the membrane membrane regions, which was also suggested previously (13). As seen from the compliance curve in Fig. 3, the 4-nN loading force led to a linear regime that indicates the tip contact with the inner membrane.

S2. SEM analysis

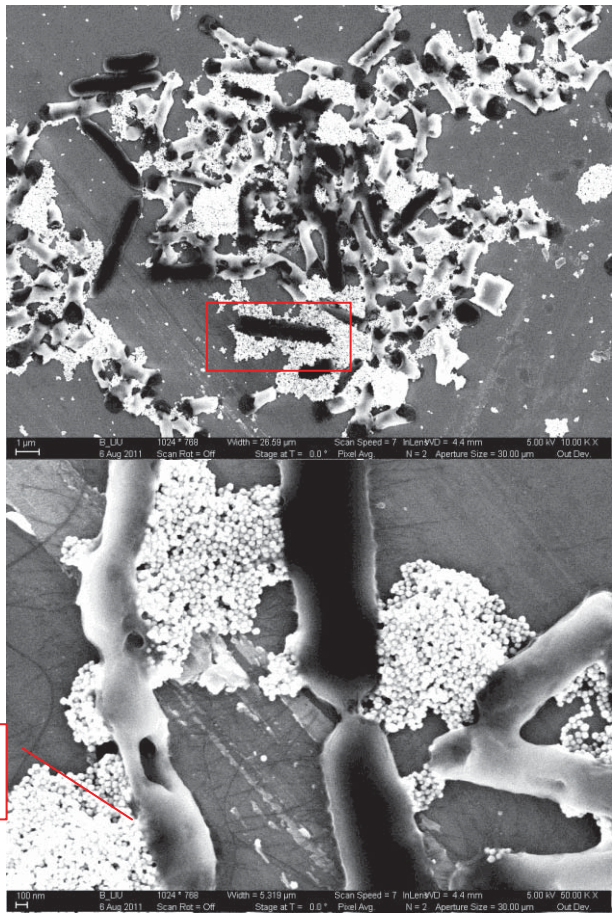

Fig. S1 SEM images of *E. coli* cells with adsorbed hematite NPs. The enlarge area of the red box is also shown in Fig. 1c.

S3. Young's modulus calculation using Hertz model

The hardness of the cells can be evaluated by the Hertz model as expressed below:

$$F = \frac{4\sqrt{R_c}}{3}\frac{E}{1-v^2}\delta^{3/2} \quad \text{(S1)}$$

where F is the loading force exerted by the tip on the surface (nN), R_c is the radius of tip curvature (approximately 20 nm as provided by the manufacture), E is the reduced Young's module of *E. coli* cells (Pa), v is the Poisson's ratio (usually set to 0.5) (3, 10), and δ is the indentation (nm). The calculated Young's module of *E. coli* cells was in the range of 52.7 kPa to 0.38 MPa, which is lower than the reported values of ~25 MPa (1, 14). The discrepancy could be ascribed to the uncertainties in the radius of the tip (usually varies with different batches of manufacturing) and in the measurement indentation.

S4. Electrophoretic mobility (EPM) measurement and PSD changes over different sorption time

Because the von Smoluchowski equation is valid for particles with uniform surface charge density, which is not true for bacteria, and moreover, the exact location of the shear plane for *E. coli* cells is hard to determine. Therefore, the EMP measurement is directly presented here in addition to zeta potentials and again, the EMP values of *E. coli* cells were not significantly different over different exposure time. A detailed interpretation of the EPM changes is difficult and beyond the scope of this study. However, it is clear that the gradual increase in EPM is probably caused by the increase of the global electrostatic charge due to the progressive coverage of NPs (5).

Table S1 EPM measurements

	Hematite NPs in PBS	*E. coli* cells in PBS	1 min exposure	5 min exposure	15 min exposure	45 min exposure
EPM, μm/s/(V/cm)	-3.78±2.37	-0.32±0.00	-2.16±1.28	-1.73±1.23	-2.27±1.3	-1.97±1.23

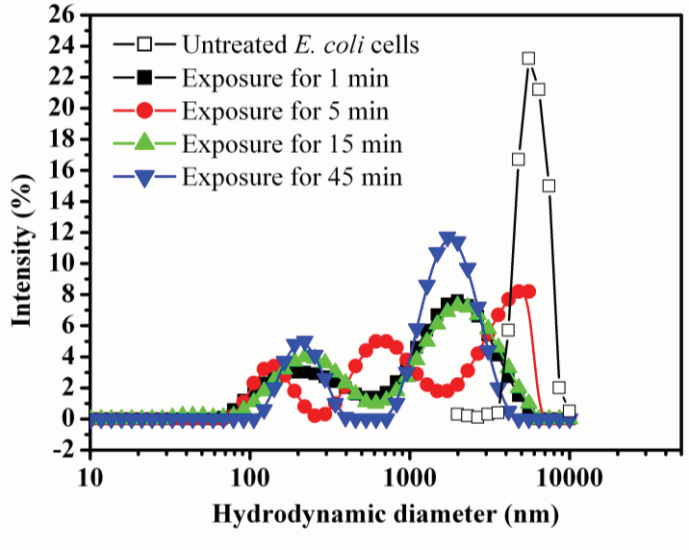

Fig. S2 Modality of PSD of the bacterial suspension at different exposure or adsorption times.

S5. Histogram of surface potential distribution of hematite NPs.

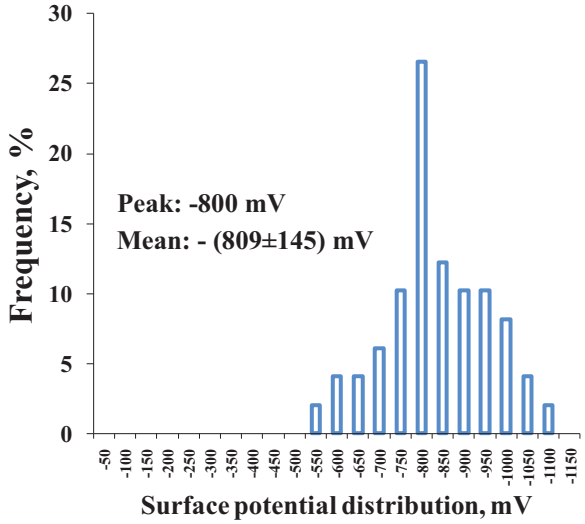

Figure S3. Histogram of the surface potential distribution measured from 50 NPs randomly chosen from Figure 5b.

S6. More images of *E. coli* cells using KPFM

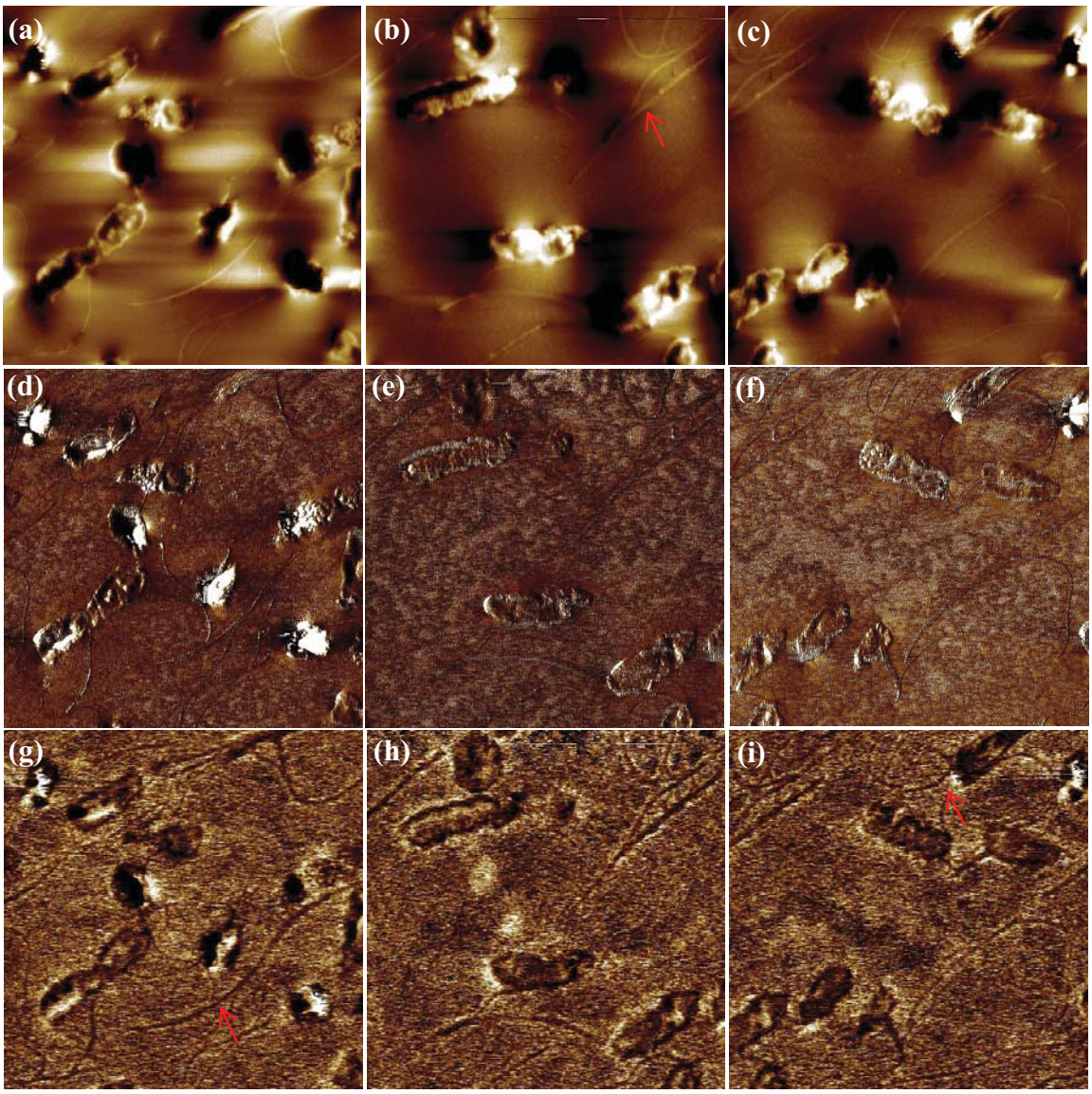

Figure S4. AFM images of *E. coli* cells. (a)-(c) are topography, (d)-(f) are phase, and (g)-(h) are surface potential images. The left column images were taken after drying for approximately 15 min; the middle column, 30 min; and the right column, 45 min. The scan area of each image is 5 μm × 5 μm. The red arrows point at a tail-like flagella.

S7. Correlation between adsorbed mass of hematite NPs and surface potentials of *E. coli* cells

As discussed previously, the surface potential decrease of *E. coli* cells should be caused by the adsorption of hematite NPs. Detailed adsorption kinetics of hematite NPs on *E. coli* cells has been investigated previously (15). Here we further used KPFM to determine the surface potentials of *E. coli* cells by randomly selecting 10 positions in the cell surface at different exposure time and then obtained the average surface potentials. Figure S5 plotted the average surface potentials at different exposure time versus the estimated corresponding mass of hematite NPs per *E. coli* surface area. The surface area that was available for hematite adsorption was estimated as follows: a single *E. coli* cell has 2.5×10^{-13} g volatile suspended solid (VSS) and a volume of 6×10^{-12} m^2 (8). In each test tube, approximately 0.1 mg/ml *E. coli* cells were dispersed in a total volume of 10 ml suspension; thus, approximately 1 mg *E. coli* cells were present in each test tube, corresponding to 4.0×10^{9} cells and 0.024 m^2 surface area that is available for the adsorption of hematite NPs. With the quantification of hematite loss in the aqueous phase of the 10-ml test tube, we could determine the adsorbed mass of hematite divided by the total surface area (0.024 m^2). Apparently, as the hematite NP adsorbed on the cell surfaces, the average surface potential dropped significantly in a non-linear fashion.

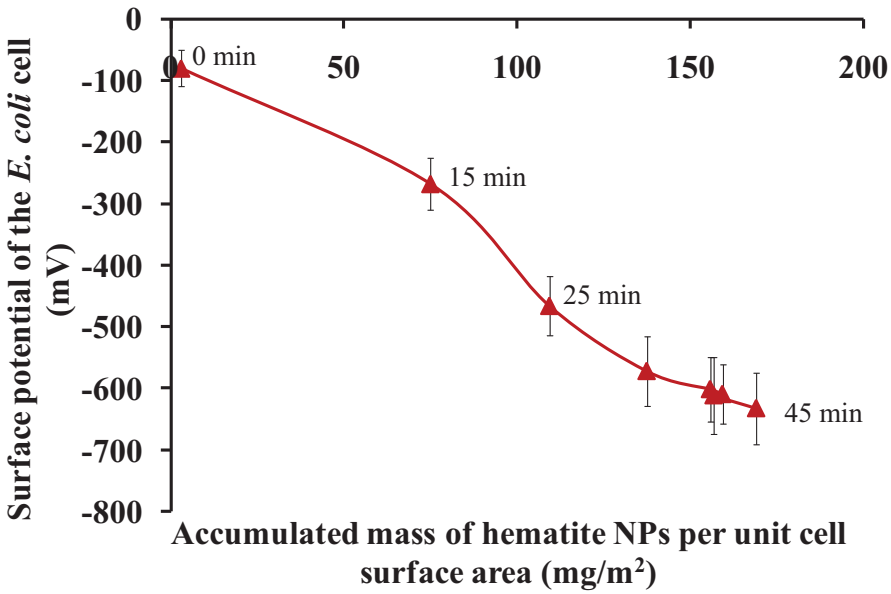

Figure S5. The accumulated mass of hematite NPs on the unit surface area of the cell versus the surface potentials of the *E. coli* cells at different exposure times. All data points are averages from the surface potential measurements on different positions of 15 hematite-treated cells, and error bars represent standard deviation.

References

1. **Boulbitch, A., B. Quinn, and D. Pink.** 2000. Elasticity of the rod-shaped Gram-negative eubacteria. Phys. Rev. Lett. **85:**5246-5249.

2. **Brayner, R., R. Ferrari-Iliou, N. Brivois, S. Djediat, M. F. Benedetti, and F. Fievet.** 2006. Toxicological impact studies based on *Escherichia* coli bacteria in ultrafine ZnO nanoparticles colloidal medium. Nano Lett. **6:**866-870.

3. **Butt, H.-J., B. Cappella, and M. Kappl.** 2005. Force measurements with the atomic force microscope: Technique, interpretation and applications. Surf. Sci. Rep. **59:**1-152.

4. **Che, C. M., C. N. Lok, C. M. Ho, R. Chen, Q. Y. He, W. Y. Yu, H. Z. Sun, P. K. H. Tam, and J. F. Chiu.** 2006. Proteomic analysis of the mode of antibacterial action of silver nanoparticles. Journal of Proteome Research **5:**916-924.

5. **Duval, J. F. L., and H. Ohshima.** 2006. Electrophoresis of diffuse soft particles. Langmuir **22:**3533-3546.

6. **Huang, Z., X. Zheng, D. Yan, G. Yin, X. Liao, Y. Kang, Y. Yao, D. Huang, and B. Hao.** 2008. Toxicological effect of ZnO nanoparticles based on bacteria. Langmuir **24:**4140-4144.

7. **Li, M., L. Zhu, and D. Lin.** 2011. Toxicity of ZnO nanoparticles to *Escherichia* coli: mechanism and the influence of medium components. Environ. Sci. Technol. **45:**1977-1983.

8. **Madigan, M. T., J. M. Martinko, P. V. Dunlap, and D. P. Clark.** 2000. Brock Biology of Microorganisms, 9th ed. Benjamin Cummings

9. **Morones, J. R., J. L. Elechiguerra, A. Camacho, K. Holt, J. B. Kouri, J. T. Ramirez, and M. J. Yacaman.** 2005. The bactericidal effect of silver nanoparticles. Nanotechnology **16:**2346-2353.

10. **Radmacher, M., M. Fritz, J. P. Cleveland, D. A. Walters, and P. K. Hansma.** 1994. Imaging Adhesion Forces and Elasticity of Lysozyme Adsorbed on Mica with the Atomic-Force Microscope. langmuir **10:**3809-3814.

11. **Shah, S. I., J. Thiel, L. Pakstis, S. Buzby, M. Raffi, C. Ni, and D. J. Pochan.** 2007. Antibacterial properties of silver-doped titania. Small **3:**799-803.

12. **Velegol, S. B., and B. E. Logan.** 2002. Contributions of bacterial surface polymers, electrostatics, and cell elasticity to the shape of AFM force curves. Langmuir **18:**5256-5262.

13. **Volle, C. B., M. A. Ferguson, K. E. Aidala, E. M. Spain, and M. E. Núñeza.** 2008. Quantitative changes in the elasticity and adhesive properties of *Escherichia coli* ZK1056 prey cells during predation by Bdellovibrio bacteriovorus 109J. Langmuir **24:**8102-8110.

14. **Yao, X., M. Jericho, D. Pink, and T. Beveridge.** 1999. Thickness and Elasticity of Gram-Negative Murein Sacculi Measured by Atomic Force Microscopy. J. Bacteriol. **181:**6865-6875.

15. **Zhang, W., B. Rittmann, and Y. Chen.** 2011. Size effects on adsorption of hematite nanoparticles on *E. coli* cells. Environ. Sci. Technol. **45:**2172-2178.